RSC Advances

This is an *Accepted Manuscript*, which has been through the Royal Society of Chemistry peer review process and has been accepted for publication.

Accepted Manuscripts are published online shortly after acceptance, before technical editing, formatting and proof reading. Using this free service, authors can make their results available to the community, in citable form, before we publish the edited article. This *Accepted Manuscript* will be replaced by the edited, formatted and paginated article as soon as this is available.

You can find more information about *Accepted Manuscripts* in the Information for Authors.

Please note that technical editing may introduce minor changes to the text and/or graphics, which may alter content. The journal's standard Terms & Conditions and the Ethical guidelines still apply. In no event shall the Royal Society of Chemistry be held responsible for any errors or omissions in this *Accepted Manuscript* or any consequences arising from the use of any information it contains.

ROYAL SOCIETY OF CHEMISTRY

www.rsc.org/advances

Please do not adjust margins

RSC Advances

ARTICLE

Carbon nanotubes growth on piezoelectric AlN films: influence of catalyst underlayers

Received 00th January 20xx,
Accepted 00th January 20xx

DOI: 10.1039/x0xx00000x

www.rsc.org/

T. Mirea,[a] J. Olivares,[a] M. Clement,[a] M. DeMiguel-Ramos,[a] J. de Frutos,[a] J. Sangrador[a] and E. Iborra[a]

Carbon nanotubes (CNTs) growth on piezoelectric AlN substrates has appeared to be important in sensing purposes using acoustic technology. CNT forests can act as sensing layers with high surface active area. We study such growth by using Fe as active catalyst and Ti, Cr and Al as catalyst underlayers. All underlayers enable CNT growth at temperatures ranging from 450°C to 650°C. Whereas Fe alone and Ti/Fe or Cr/Fe stacks provide multi-walled CNT with high defect content, Al/Fe stack yields CNT forests with G to D peak ratios up to 9.2 with single and double-walled CNT content. The low surface energy of Al and its roughness are key factors in this successful growth. These results are not only useful for sensing applications but can also place AlN as an alternative insulating substrate for CNT growth.

1. Introduction

Carbon allotropes have attracted the attention of the scientific community during the last decades due to their technological properties and the possibilities they offer for unique materials development with different structures.[1,2] In particular, carbon nanotubes (CNTs) are one of the most attractive carbon-based structures due to their outstanding properties.[3] They show high electrical and thermal conductivities, high in-axis elastic constant, low mass density and the lowest diameter a cylinder-like structure can present. These characteristics make them suitable for a large variety of applications. For instance, due to their good electrical conductivity, CNTs are being considered as electric interconnects in micro and nano-electronics.[4] On the other hand, their high surface to volume ratio and the possibility of being easily functionalized, hold out the prospect of using CNTs as sensing layers in different types of sensors.[5-9] In most of these cases CNTs are either used in a tangled-like form or composing a dispersion or composite. CNTs in forest structures (i.e. vertically-aligned) acting simultaneously as top electrode and sensing layer have been proposed[10] to boost their application in gravimetric electroacoustic sensors. CNT forests with high area density guarantee high effective surface area for sensing purposes and high conductivity, which reduces the electrical resistance of the forest[11] and is essential for the good performance of electroacoustic resonators.[10]

To fulfil the simultaneous application, CNT forests have to be grown directly and surface-bonded to the piezoelectric film of the resonators. The basics of gravimetric acoustic sensors is the dependence of the resonant frequency with the mass of the device. An added mass implies a decrease of this frequency. The sensing layer and the bonded targeted species should form part of the resonator and jointly move as a whole when the device resonates. This implies that the adhesion of CNTs to the substrate must be tight.

CNT forests are typically grown using the chemical vapour deposition (CVD) technique consisting on the thermal decomposition of gaseous hydrocarbons activated by catalysis.[12,13] The growth process is divided in two stages: 1) formation of catalytic nanoparticles (NPs) and 2) growth of CNTs. We can grow single-walled nanotubes (SWCNTs) or multi-walled nanotubes (MWCNTs). Additionally, either a base-growth mechanism, where the catalytic NP remains anchored to the substrate, or a tip-growth mechanism, where the NP is pushed off the substrate and placed at the tip of the nanotube, can take place. The first one is preferred if a tight adhesion between CNTs and substrate is desired.

Two of the most widely used piezoelectric materials in high frequency acoustic resonators are AlN and ZnO. CNTs have been grown successfully on insulating materials, such as Al_2O_3 or SiO_2.[14,15] However, few studies have reported on the growth of CNTs on piezoelectric materials.[10,16,17] Most of these studies report on the growth of forests essentially composed of MWCNTs, whereas SWCNTs are rarely obtained.[17] Since we are pursuing high active surface area for functionalization, high area density forests of SWCNTs would be more desired.[18]

The NP nature and size combined with the CNT growth parameters define the main characteristics of the nanotube forests (number of walls, area density, and nanotubes length). Catalytic NPs are created by annealing a thin layer of catalytic metal in a controlled atmosphere. The factors that most influence the formation of NPs are related to the catalyst-substrate interaction, namely de-wetting of the catalyst from

[a] GMME-CEMDATIC, ETSIT. Universidad Politécnica de Madrid, Madrid, Spain. E-mail: enrique.iborra@upm.es
†Electronic Supplementary Information (ESI) available:
See DOI: 10.1039/x0xx00000x

RSC Advances Accepted Manuscript

Please do not adjust margins

the substrate, surface diffusion of NP across the substrate, bulk diffusion into the substrate, or a combination of all.[19] The successful growth of CNTs on insulating materials is associated to a low bulk diffusion of the catalyst and an adequate de-wetting from the substrate, which is in turn related to its surface energy. Ideally, the substrate surface energy should be lower than that of the catalyst, so de-wetting can easily proceed allowing NP formation.[20] The most active catalytic materials for CNT growth have been proven to be metals like Fe, Ni and Co,[21] with surface energies lying between 2.0 J/m^2 and 2.8 J/m^2.[22] The surface energies of the most common insulating substrates (SiO_2 or Al_2O_3) are around 0.1 J/m^2, considerably lower than those of the mentioned catalysts, which explains their successful use as CNT substrates. However, even if de-wetting easily proceeds on insulating materials, surface diffusion and coalescence of NPs should be also controlled by stabilising them after formation. Effective methods to reduce the mobility of NPs and to enhance their area density are the use of catalyst underlayers,[23,24] co-catalysts,[17,25] or more complex structures based on sandwich-like or multi-cycle techniques.[4,26]

In this paper we study the growth of CNT forests on piezoelectric AlN films with pure (00·2) orientation (*c*-axis of the wurtzite structure perpendicular to the surface). We use Fe as catalyst and C_2H_2 as carbon source. Theoretical calculations of the surface energy of AlN wurtzite structures yield values of around 5.84 J/m^2,[27] which is considerably high considering the insulating character of AlN. This ab-initio high surface energy of AlN suggests using the same technique we employed in a previous work that enabled growing highly packed vertically-aligned SWCNTs on pure Ir and Mo metallic films.[28] This consists in using thin Al underlayers, to prevent NP surface diffusion, and temperatures for NP formation lower than those used for nanotubes growth, preventing bulk diffusion of the catalyst into the metallic substrate. In the present work, we investigate the influence of Al, Ti and Cr underlayers in the growth of CNT forests on AlN. We focus on the influence of the surface energies of the underlayers and the temperature used for NP formation. The CNT forest with the best quality is obtained with the Al underlayer.

2. Experimental methods

The piezoelectric substrates consist in *c*-axis-oriented AlN wurtzite films (1 to 2 µm-thick) sputtered on Ir thin films acting as bottom electrode in bulk acoustic wave resonators.[29] The AlN films are covered with a thin Fe layer or an underlayer/Fe stack deposited in sequence (without breaking vacuum in the deposition system) by thermal evaporation at a base pressure lower than 2×10^{-5} Pa. Three materials are tested as underlayers – Ti, Cr and Al. Their thicknesses (optimised) are 2 nm for Ti and Cr, and 8 nm for Al. The optimised thickness of the Fe catalyst film is 1.5 nm. All films are deposited at constant deposition rate controlled by a quartz microbalance. The deposition rate was previously calibrated by assessing the thickness of test samples using x-ray reflectance (XRR) measurements. These measurements were also used to extract the actual density of evaporated Fe films exposed to air.

We use a cold-wall low pressure CVD (LPCVD) system for CNT growth. After the evaporation of the underlayers and the Fe films, samples are transferred (air transfer) to the LPCVD system and placed onto a pyrolithic carbon heater. The temperature of the samples is controlled by means of a programmable temperature controller using the signal of a *K*-type thermocouple directly sit atop the sample. We use NH_3 as reducing gas and C_2H_2 as carbon source, which is referred to be the best choice for SWCNT growth.[26] We ensure the cleanliness of the chamber by repeating high purity-N_2 purge/vacuum cycles prior to CNT growth process. Once cleanliness is achieved, NH_3 is fed into the chamber at a rate of 50 sccm until a pressure of 18 Pa is reached. NH_3 supply is kept constant during the entire process. A simple scheme of the growth process is depicted in Fig. 1. The first stage of the process consists in NP formation. We heat the samples at 200°C/min to a temperature T_{NP} (450°C, 550°C or 650°C) keeping it for 5 minutes. After NP formation, we rise the temperature to T_{CNT} (650°C) at a rate of 100 °C/min. Once T_{CNT} is reached we start CNT growth by adding C_2H_2 at a rate of 50 sccm to form a 1:1 NH_3:C_2H_2 admixture at a pressure of 33.3 Pa. These conditions are maintained for 10 minutes. Finally the samples are cooled down in vacuum.

We use atomic force microscopy (AFM) measurements to study the NPs appearance. To perform these measurements we take the samples out of the chamber after NP formation and before CNT growth stage. Once CNT are grown, we use scanning electron microscopy (SEM) to assess the forests heights by examining their cross section in cleaved samples. The CNT structure is assessed by Raman spectroscopy using a 532 nm wavelength laser.

3. Results and discussion

We have tested CNT growth using Fe as catalyst alone and combined with the three mentioned underlayers. We achieve CNT growth with all underlayers and for all T_{NP}. Each catalytic system provides CNT forests with different qualities. In each case (Fe, Cr/Fe, Ti/Fe and Al/Fe) the CNT forests are similar (height and structure) independently of T_{NP} (450°C, 550°C or 650°C), with slight improvement (less defects observed by

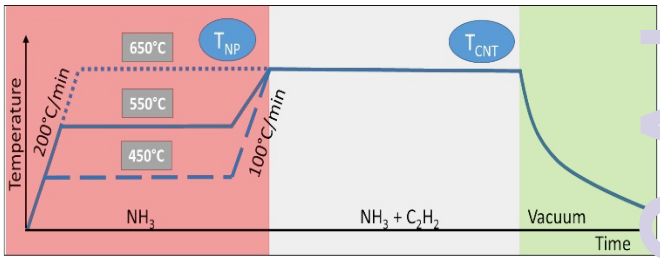

Fig 1. Stages of CNT growth process: 1) NPs formation, 2) CNT growth and 3) final cooling down.

RSC Advances Accepted Manuscript

Raman spectroscopy and increased height) for the highest T_{NP} = 650°C. For this reason we will focus the comparison and discussion on the results obtained using this temperature for all cases. We confirm base-growth mechanisms for all combinations by manually removing the CNTs and growing them again.

In Fig. 2 we show AFM measurements of NPs formed at T_{NP} = 650°C for all catalytic systems. When analysing the AFM images one should consider two facts. Firstly, the image that the equipment obtains is a convolution of the AFM tip diameter (5 nm) and the NPs diameter. Thus, we do not observe the exact NP dimensions, but an overestimation. To complement Fig. 2 we present in Fig. 3 the roughness of the same samples, namely their vertical dimensions, before and after NP formation. From both figures we can see that after annealing, the NPs formed from Cr/Fe have the largest appearance in both lateral and vertical dimensions, and the NPs obtained from Al/Fe are relatively taller, more defined and denser than the ones formed from Fe or Ti/Fe. Hence, Al/Fe catalytic system provides the NPs with the best quality. This is in good agreement with Fig. 4, where SEM images of CNT forests grown at T_{CNT} = 650°C from NPs similar to those from Fig.2 are presented. Al/Fe NPs allow the growth of the tallest and most packed forest. Secondly, it should be considered that the real dimensions of the NPs when CNT growth starts are smaller. The AFM measurements are performed on samples with oxidised NPs (air transfer). From XRR measurements (not presented here) we extract a 66% density of that of pure Fe, for the as-deposited

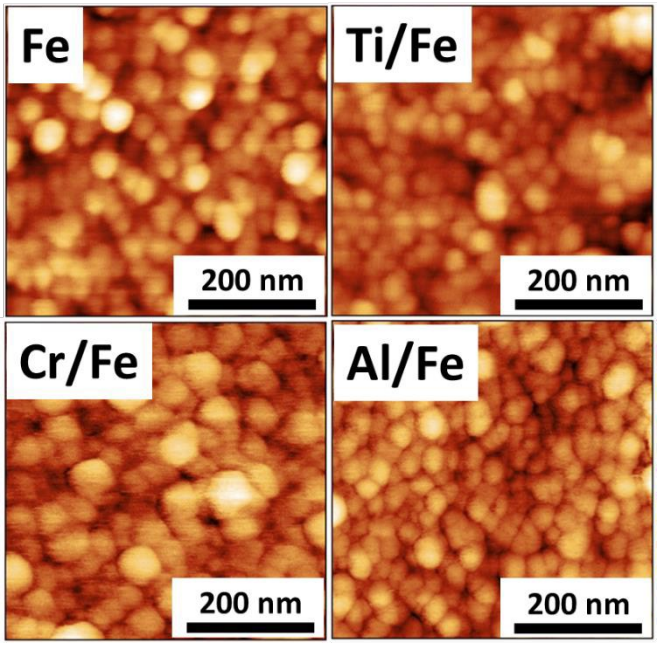

Fig 2. AFM images of AlN surfaces containing NPs of samples using 1.5 nm for the Fe catalyst, 2 nm for both Ti and Cr underlayers, and 8 nm for the Al underlayer. NPs are formed after 5 min at T_{NP} = 650°C in NH_3 (18 Pa) and removed from the chamber just before C_2H_2 introduction.

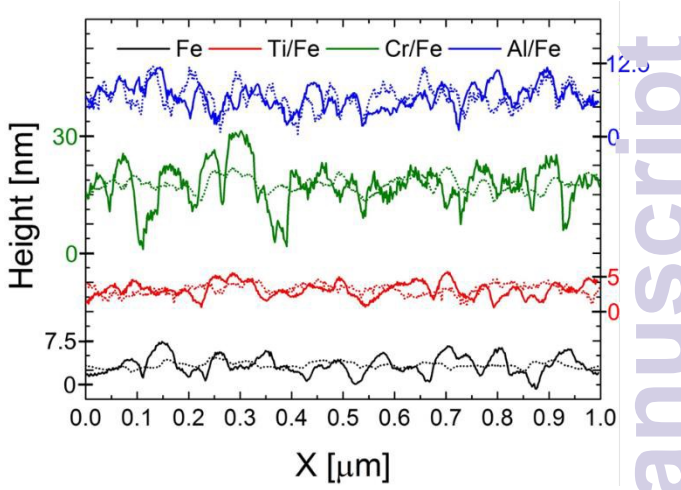

Fig 3. Roughness of 1.5 nm of Fe, 2 nm/1.5 nm of Ti/Fe, 2 nm/1.5 nm of Cr/Fe and 8 nm/1.5 nm of Al/Fe. As-deposited film (dotted lines), and after reducing atmosphere treatment for 5 min at T_{NP} = 650°C (solid lines).

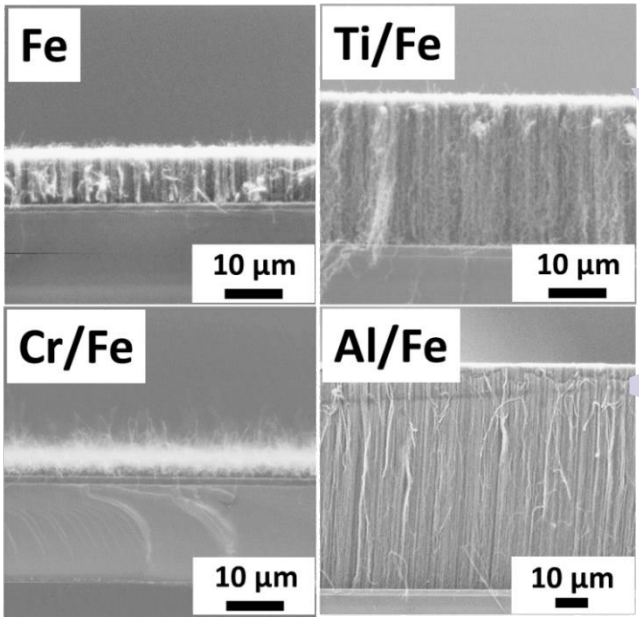

Fig 4. SEM images of CNTs grown from samples with Fe, Ti/Fe, Cr/Fe and Al/Fe layers and same NPs as in Fig. 2 (without breaking process/vacuum). CNTs are grown after 10 min at T_{CNT} = 650°C in the 1:1 NH_3:C_2H_2 admixture (33.3 Pa). The heights of the forests are 9 µm, 4.5 µm, 21 µm and 63 µm for the Fe, Cr/Fe, Ti/Fe and Al/Fe stacks, respectively.

Fe layers, indicating great oxygen content. It is worth mentioning that CNTs can also grow on samples with NPs that have experienced air contact after being formed in NH_3 (i.e. were taken out of the system before CNT growth stage. After loading them again in the LPCVD system, NH_3 reduces the NPs removing oxygen content. The quality of these CNTs is as good as the ones grown on NPs without air contact.

RSC Advances Accepted Manuscript

Raman spectra from Fig. 5 reveal that with Fe, Ti/Fe and Cr/Fe we can only obtain forests containing mainly MWCNTs with high defect content (G to D ratios close to 1). However, we attribute the Raman spectrum of CNTs grown using Al/Fe to an important presence of SWCNTs and possibly double-walled CNT (DWCNTs). The features that evidence this are: strong RBM peaks, high G to D ratio (around 9.2), G band splitting, presence of M and iTOLA peaks and shift to lower energies of the single component of the 2G peak.[26,30,31]

A combination of several effects can explain the successful growth of CNTs on piezoelectric AlN films. AlN is a rough substrate due to its columnar grain structure. This has been proven to be useful since it provides sinks for NPs, inhibiting their coalescence due to surface diffusion.[16,23] Fe has proven to favour CNT growth on AlN since it tends to oxidise slightly;[32] moreover, specific bonds between Fe-N and Fe-Al occur, offering NP immobilisation.[16,33] Additionally, the roughness of an Al underlayer increases the amount of sinks for NPs and favour their formation and stabilisation in smaller dimensions.

The profile lines of the AFM images presented in Fig. 3 set clear that as-deposited Al/Fe already provides increased roughness compared to the other cases. After annealing, while Al/Fe conserves the initial roughness allowing and immobilising small NPs, too large and less defined NPs are observed for the other cases.

Although surface roughness helps low-size NP formation, a more reliable explanation on the effect of each underlayer can be given in terms of their surface energy. The three different underlayers have different surface energies and reflect the influence of this physical property on NP formation. The theoretical surface energy of piezoelectric AlN films with wurtzite structure (5.84 J/m^2) is greater than that of Fe (2.4 J/m^2) or the underlayers (3.5 J/m^2, 2.6 J/m^2 and 1.1 J/m^2 for Cr, Ti and Al, respectively)[22]. Considering this, one might think that de-wetting using only Fe can hardly be achieved. However, the fact that AlN has been in contact with air before catalyst deposition suggests that oxygen incorporation to the surface is possible.[16] This reduces the surface energy of the AlN substrate, since Al-O compounds have very low surface energy (such as 0.1 J/m^2 for Al_2O_3).[20] The resulting surface energy has not necessarily to be as low as the Al_2O_3 one since a short exposure to air does not guarantee the formation of this compound. Rather than Al_2O_3 it forms Al-N-O compounds. To check the surface energy of AlN exposed to air, we perform a simple test to compare it to that of Al_2O_3 and Ir. We put on the three surfaces a droplet of DI water (identical amount) and compare their shapes (Fig. 6). The picture reveals that de-wetting of the droplet from the AlN substrate proceeds harder than from Al_2O_3, since the contact angle between the droplet and the surface is smaller, but easier than from Ir. The greater the surface energy of the substrate, the easier to achieve complete wetting of the liquid.[34] This simple test does not provide quantitative values for the surface energies, but confirms that the surface energy of wurtzite AlN exposed to air is greater than 0.1 J/m^2 and smaller than 3.0 J/m^2, hence lower than the theoretical value of 5.84 J/m^2.

A more realistic scheme of the four situations we are dealing with, namely AlN/Fe, AlN/Cr/Fe, AlN/Ti/Fe and AlN/Al/Fe stacks is depicted in Fig. 7. Here we are considering the estimated surface energy of AlN exposed to air (textured film on top of the AlN represents possible Al:O or Al:N:O compounds) and the corresponding theoretical values of underlayers and catalyst. The biggest NPs and worst CNT forests are obtained with Cr underlayer, which has a surface energy higher than that of Ti and Al. The reason could be the fact that its de-wetting from the AlN substrate proceeds easily and forms big islands (for all T_{NP}) without providing small sites for the formation of Fe NPs. These islands are bigger than the corrugation offered by the AlN surface. Thus Cr/Fe NPs move easily across the surface and Fe

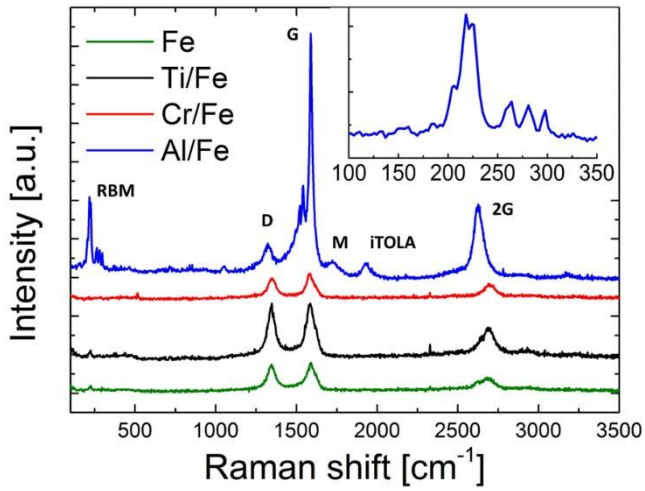

Fig 5. Raman spectra of the CNT forests from Fig. 4 grown using Fe, Ti/Fe, Cr/Fe and Al/Fe, for T_{NP} =T_{CNT} = 650°C. CNTs grown from Al/Fe present a G to D ratio of around 9, while the other cases show a value around 1. The inset shows in detail the RBM peaks of the Al/Fe spectrum, fingerprint proving the presence of SWCNTs and/or DWCNTs.

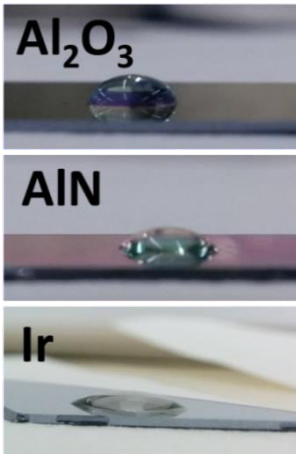

Fig 6. Comparison between Al_2O_3 (0.1 J/m^2) – AlN – Ir (3.0 J/m^2) surface energies using a droplet of DI water. Wurtzite AlN surface energy lies between 0.1 J/m^2 – 3.0 J/m^2.

RSC Advances Accepted Manuscript

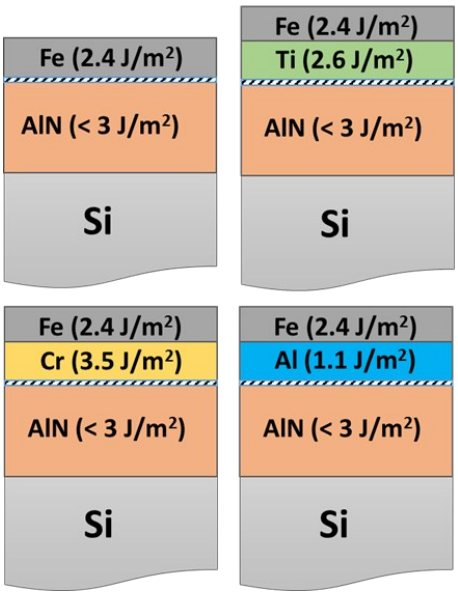

Fig 7. Scheme of theoretical surface energies for all underlayers-catalyst combinations.

NPs are not stabilised. Ti offers lower surface energy than Cr, hence de-wetting from the AlN substrate proceeds with more difficulty preventing the formation of very big islands.

The case of Ti/Fe can be applied to the case of Fe alone, as the results obtained for both cases are very similar. Finally, Al has the lowest surface energy, which does not allow easy de-wetting from the AlN substrate, but high enough as to provide small nucleation sites for the formation of very small Fe NP.

The introduction of Al in the catalyst stack has already proven to promote SWCNT growth on other substrates.[23] Although CNT growth on AlN using only Fe is possible due to Fe-N and Fe-Al interactions,[16] placing an Al underlayer between Fe and AlN, provides increased roughness and less mobility for Fe NPs stabilizing them . This favours the growth of denser and with higher quality forests than when using other underlayers as Ti or Cr.

4. Conclusions

CNT growth on piezoelectric AlN is possible using Fe as catalyst. However the forests obtained using only Fe contain mainly MWCNTs with high defect content. By using a catalyst underlayer we can stabilise the Fe NPs and achieve smaller dimensions. Ti and Cr underlayers do not provide smaller NPs than Fe alone, hence the CNTs are similar in quality containing mainly MWCNTs as well. On the contrary, Al underlayer provides the highest CNT qualities. The forests grow taller, more packed, with high quality and with SWCNTs and DWCNTs content. This is achieved due to the Al low surface energy and its increased surface roughness.

The successful growth of tall, dense and high quality CNT forests on AlN is not only useful for sensing purposes in acoustic devices. AlN can appear to be a new alternative to other common substrates used for CNTs growth.

Acknowledgements

This work was partially supported by the European Commission through the 7th Framework Programme by the Rapta- Diag project HEALTH-304814 (www.raptadiag.eu/) and by the Ministerio de Economía y Competitividad del Gobierno de España through project MAT2013-45957R.

Notes and references

1 A. Hirsch, *Nature Materials*, 2010, **9**, 868–70.
2 M. Mecklengurg, A. Schuchardt, Y. K. Mishra, S. Kaps, R. Adelung, A. Lotnyk, L. Kienle and K. Schulte, *Adv. Mater*, 2012, **24**, 3486–90.
3 M.S. Dresselhaus, G. Dresselhaus and Ph. Avouris, *Carbon nanotubes: Synthesis, Structure, Properties, and Applications*, Springer Science & Business Media, 2001.
4 S. Esconjauregui, M. Fouquet, B. C. Bayer, C. Ducati, R. Smajda, S. Hofmann and J. Robertson, *ACS Nano*, 2010, **12**, 7431–7436.
5 C. Zuniga, M. Rinaldi, S. M. Khamis, A. T. Johnson and G. Piazza, *Appl Phys Lett*, 2009, **94**, 223122.
6 Llobet, *Sens Actuator B Chem*, 2013, **157**, 1–7.
7 .Wang nanocomposites 2014
8 L. García-Gancedo, Z. Zhu, E. Iborra, M. Clement, J. Olivares, A.J. Flewitt, W.I. milne, G.M. Ashley, J.K. Luo, X.B. Zhao and J.R. Lu, *Sens Actuator B Chem*, 2011, **160**, 1386–93.
9 Z. Zhu, L. García-Gancedo, A.J. Flewitt, H. Xie, F. Moussy, W.I. Milne, *Sensors*, 2012, **12**, 5996–6022.
10 T. Mirea, J. Olivares, M. DeMiguel-Ramos, M. Clement, S. Esconjauregui, J. Sangrador and E. Iborra, *Carbon nanotube forests as top electrodes for AlN-based electroacoustic resonators*, IEEE International Ultrasonics Symposium Chicago, 2014.
11 J. Robertson, G. Zhong, H. Telg, C. Thomsen, J.H. Warner, G.A.D. Briggs, U. Dettlaff-Weglikowska and S. Roth, *Appl Phys Lett*, 2008, **93**, 163111.
12 M. Kumar and Y. Ando, *J. Nanosci. Nanotechnol.*, 2010, **10**, 3739–58.
13 J. Robertson, G. Zhong, S. Esconjauregui, C. Zhang, M. Fouquet and S. Hofmann, *Phys. Status Solidi B*, 2012, **249**, 2315–22.
14 G. Zhong, T. Iwasaki, K. Honda, Y. Furukawa, I. Ohdomari and H. Kawarada, *Jpn. J. Appl. Phys*, 2005, **44**, 1558–1561.
15 C. Ducati, I. Alexandrou, M. Chhowalla, G.A.J. Amaratunga and J. Robertson, *J Appl Phys*, 2002, **92**, 3299–3303.
16 B. Eren, L. Marot, R. Steiner, T. de los Arcos, M. Düggelin, D. Mathys, K.N. Goldie, V. Olivieri and E. Meyer, *Chem Phys Lett*, 2014, **609**, 82–87.
17 S. Maruyama, E. Einarsson, Y. Murakami and T. Edamura, *Chem Phys Lett*, 2005, **403**, 320–323.
18 B. Zhao, D.N. Futaba, S. Yasuda, M. Akoshima, T. Yamada and K. Hata. *ACS Nano*, 2009, **3**, 108–114.
19 A.C. Dupuis, *Prog Mater Sci*, 2005, **50**, 929–961.
20 C. Zhang, F. Yan, C.S. Allen, B.C. Bayer, S. Hofmann, B.J. Hickey, D. Cott, G. Zhong and J. Robertson, *J Appl Phys*, 2010, **108**, 1–6.
21 S. Esconjauregui, C.M. Whelan and K. Maex, *Carbon*, 2009, **47**, 659–69.
22 L. Vitos, A.V. Ruban, H.L. Skriver and J. Kollár, *Surf Sci*, 1998, **411**, 186–202.
23 L. Delzeit, B. Chen, A. Cassell, R. Stevens, C. Nguyen and M. Meyyappan, *Chem Phys Lett*, 2001, **348**, 368–374.

RSC Advances Accepted Manuscript

24 Y. Wang, B. Li, P.S. Ho, Z. Yao, L. Shi, *Appl Phys Lett*, 2006, **89**, 1–3.
25 S. Noda, H. Sugime, T. Osawa, Y. Tsuji, S. Chiashi, Y. Murakami and S. Maruyama, *Carbon*, 2006, **44**, 1414–1419.
26 G. Zhong, S. Hofmann, F. Yan, H. Telg, J.H. Warner, D. Eder, *J Phys Chem*, 2009, **113**, 17321–17325.
27 D. Holec and P.H. Mayrhofer, *Scri Mater*, 2012, **67**, 760–762.
28 J. Olivares, T. Mirea, B. Díaz-Durán, M. Clement, M. DeMiguel-Ramos, J. Sangrador, J. de Frutos and E. Iborra, *Carbon*, 2015, **90**, 9–15.
29 M. Clement, J. Olivares, E. Iborra, S. González-Castilla, N. rimmer and A. Rastogi, *Thin Solid Films*, 2009, **517**, 4673–4678.
30 W. Qian, T. Liu, F. Wei, H. Yuan, *Carbon*, 2003, **41**, 1851–1864.
31 M.S. Dresselhaus, G. Dresselhaus, R. Saito and A. Jorio, *Physics Reports*, 2005, **409**, 47–99.
32 T. de los Arcos, M.G. Garnier, P. Oelhafen, D. Mathys, J.W. Seo and C. Domingo, *Carbon*, 2004, **42**, 187–90
33 S. Esconjauregui, T. Makaryan, T.Mirea, M. DeMiguel-Ramos, J. Olivares, Y. Guo, H. Sugime, L. D'Arsié, J. Yang, S. Bhardwaj, C. Cepek, J. Robertson and E. Iborra, submitted for publication.
34 P.G. de Genes, *Rev Mod Phys*, 1985, **57**, 827–863.

RSC Advances Accepted Manuscript